Analyst

PAPER

View Article Online
View Journal | View Issue

Cite this: *Analyst*, 2014, **139**, 4073

SERS of molecules that do not adsorb on Ag surfaces: a metal–organic framework-based functionalization strategy†

Lauren E. Kreno,[a] Nathan G. Greeneltch,[a] Omar K. Farha,[ab] Joseph T. Hupp*[a] and Richard P. Van Duyne*[a]

Received 27th February 2014
Accepted 3rd June 2014

DOI: 10.1039/c4an00413b

www.rsc.org/analyst

The potential for discriminating between analytes by their unique vibrational signature makes surface-enhanced Raman scattering (SERS) extremely interesting for chemical detection. However, for molecules that weakly adsorb to non-functionalized plasmonic materials, detection by SERS remains a key challenge. Here we present an approach to SERS-based detection where a polycrystalline metal–organic framework (MOF) film is used to recruit a range of structurally similar volatile organic compounds for detection by SERS. MOF films were grown on the surface of Ag "films-over-nanospheres" (FONs), which have previously been shown to enhance Raman signals of surface adsorbates by a factor of 10^7. Upon exposing the MOF-coated FON to benzene, toluene, nitrobenzene, or 2,6-di-*tert*-butylpyridine, the MOF film traps the vapors at the FON surface, allowing the unique Raman spectrum of each vapor to be recorded. By contrast, these analytes do not adsorb to a bare FON surface and thus cannot be detected by conventional SERS substrates. Pyridine was also tested as a Ag-adsorbing control analyte. Concentration dependence and time resolved measurements provide evidence for the hypothesis that the vapors are reversibly adsorbed on the surfaces of MOF nanocrystals exposed at grain boundaries. This represents a generalized approach for confining aromatic molecules through interactions with the MOF surface, which can be applied for future SERS-based sensors.

Introduction

Surface-enhanced Raman scattering (SERS) has been widely explored as a means of chemical detection because it operates under ambient conditions, can be portable,[1,2] and has limits of detection down to the single molecule level.[3–6] Most importantly, SERS can uniquely identify molecules by their vibrational fingerprint. A principal challenge in using any surface-enhanced spectroscopy for detection purposes is localizing the molecule of interest at the enhancing surface. In SERS, the Raman signal of a molecule can be enhanced by many orders of magnitude,[7–10] but close proximity (<3–5 nm) to a plasmonic surface or nanoparticle is key. The vast majority of SERS literature focuses on molecules that strongly chemisorb to plasmonic metal surfaces at ambient temperatures. These include pyridine and other heterocyclic molecules,[11] dye molecules,[5,12,13] and thiols[14,15] used for fundamental studies of SERS as well as explosives,[15–17] pesticides,[18] drugs,[19] chemical warfare agents,[1,20,21] and pollutants[22] for SERS-based detection. In fundamental studies, it is convenient to use molecules which form dense monolayers on the particle surface, but for sensing applications, some target analytes simply do not adsorb.

To address this problem, various techniques have been developed to capture non-adsorbing molecules for SERS detection. For vapors, the sample surface often must be cooled to cause condensation of liquid or solid on the surface.[23–25] In other cases, a capture layer can be coated on the SERS-active surface to bind or partition analytes. We previously demonstrated this strategy where glucose, which does not bind to Ag, is reversibly partitioned into a mixed thiol monolayer for SERS detection in solution.[26] Carboxylic acid-terminated thiols were used to electrostatically bind cytochrome C to SERS-active surfaces.[27] We have also used alumina overlayers grown by atomic layer deposition to increase the binding of dipicolinic acid, an anthrax biomarker, on SERS substrates. In other work, Ko *et al.* used polyelectrolyte coatings to increase the adsorption of explosives deposited by drop-casting.[28] However, detection of non-adsorbing molecules in the vapor phase remains a challenge for SERS, as evidenced by the lack of literature on this subject. It is well known, for example, that many volatile

[a]*Department of Chemistry, Northwestern University, 2145 Sheridan Road, Evanston, Illinois 60208, USA. E-mail: j-hupp@northwestern.edu; vanduyne@northwestern.edu; Fax: +1 847 491-7713; Tel: +1 847 491-3504; +1 847 491-3516*

[b]*Department of Chemistry, Faculty of Science, King Abdulaziz University, Jeddah, Saudi Arabia*

† Electronic supplementary information (ESI) available: Characterization of MOF/FONs by XRD and SEM, schematic of SERS setup, adsorption and desorption of benzene in ZIF-8 by SERS, calculation of the benzene layer thickness on a bare FON, and analysis of vapor sorption by QCM. See DOI: 10.1039/c4an00413b

aromatic molecules do not adsorb to metal surfaces at room temperature[29–31] making it difficult to detect them by SERS. Nonpolar alkanethiol monolayers have been used to promote the adsorption of volatile aromatic molecules like benzene and toluene,[32] but cooling of the sample may still be required to observe the analyte spectra.[33] An alternative approach to achieve detection at room temperature is to utilize a sorptive polymer on the surface of the nanoparticles[34] or the nanoparticle support.[35] In this work, we present a new approach to room temperature detection by functionalizing a Ag SERS-active surface with a metal–organic framework (MOF) film to promote the adsorption of volatile organic compounds (VOCs) that would not normally adsorb to a Ag surface under ambient conditions.

MOFs are hybrid organic–inorganic materials composed of metal cation or cluster nodes connected by multitopic organic linkers to form crystalline networks.[36–38] Many MOFs are permanently porous and can have internal surface areas up to ~7000 $m^2\ g^{-1}$ (ref. 39) making them ideal for varied applications including fuel storage,[40,41] carbon capture,[42] gas separations,[43] catalysis,[44,45] and sensing.[46,47] Primarily, they are interesting for sensing because their highly porous nature allows MOFs to store gases and vapors at much higher concentrations than are present in the atmosphere. For example, we previously demonstrated that thin films of MOFs can be deposited on the surface of plasmonic nanoparticles for use as refractive index-based sensors due to the MOF preferentially concentrating CO_2.[48] Extending this concept to SERS, Sugikawa *et al.* recently demonstrated that it is possible to measure SERS spectra of liquid solvent filling the pores of a MOF by embedding randomly dispersed Au nanorods in the MOF crystals.[49] The combination of MOFs with SERS-active structures has not yet been extended to vapor or gas sensing.

Rather than embedding nanoparticles in MOFs, we have taken a different approach aimed at maximizing the interface between the plasmonic surface and the MOF. MOF thin films were used to functionalize the surface of SERS-active structures dubbed Ag "films-over-nanospheres" (FONs),[50–52] which are known to have very uniform SERS enhancement of $>10^7$.[53] Here we present our findings with the well-studied MOF ZIF-8 ($Zn(mIm)_2$, mIm = 2-methylimidazolate).[54] Surprisingly, we have found that films of ZIF-8 are capable of recruiting a range of volatile aromatic vapors to the surface of an otherwise non-adsorptive FON. These results were initially unexpected because the kinetic diameters of these molecules are larger than the size of the aperture leading to the ZIF-8 pore,[55] and as such they are not able to access the micropores of the MOF. Nonetheless, we demonstrate that these molecules (benzene, toluene, pyridine, nitrobenzene, and 2,6-di-*tert*-butylpyridine) are trapped by the film through apparent favorable but reversible interactions with the MOF. Most of these vapors do not adsorb to non-functionalized metal surfaces, so the MOF film plays a crucial role in confining molecules in the nanoscale hot spots of the FON. This work represents an entirely new approach to vapor-phase SERS sensing, and the fabrication of the MOF/FON (ZIF-8-coated Ag FON) architecture provides a step towards the development of a true MOF-based SERS sensing device for volatile chemicals.

Experimental

All reagents were purchased from Sigma Aldrich and all solvents were purchased from VWR and used as received, unless otherwise specified.

Fabrication of plasmonic substrates

Ag FONs were prepared using a previously reported fabrication method.[50,53] Glass microscope coverslips (18 mm, Fisher Scientific) were cleaned by immersing in piranha solution ($3:1\ H_2SO_4:H_2O_2$) for one hour. **Caution**: Piranha solution is extremely corrosive, and appropriate personal protective equipment should be used during handling. Clean coverslips were rinsed with copious amounts of deionized water. The coverslips were then treated with a basic solution by sonicating for one hour in $5:1:1\ H_2O:NH_4OH:H_2O_2$ followed by rinsing with deionized water. Next, ~4–5 μL of silica nanospheres in water (390 nm or 590 nm diameter, 10 wt%, Bangs Labs) were drop-coated on top of each wet cover slip and the cover slips were rotated in a circular motion to distribute the solution homogeneously. Allowing the substrate to dry slowly in air produced a multi-layered hexagonally close-packed array of nanospheres. 200 nm of Ag (Kurt J. Lesker Co.) was thermally evaporated in vacuum (5×10^{-6} torr) at a rate of 1–2 Å s^{-1} atop these nanosphere arrays to produce FON SERS-active surfaces.

Growth of ZIF-8 on FON

ZIF-8 was grown on the FONs at room temperature using a previously reported procedure.[56] 5 mL of 25 mM $Zn(NO_3)_2$/methanol was added to 5 mL of 50 mM 2-methylimidazole/methanol in a vial and mixed by shaking for 30 s. A FON substrate was immersed in the solution leaning against a microscope slide to stand it upright. After several minutes the growth solution turned iridescent and became increasingly opaque white as ZIF-8 nanocrystals formed in solution. After 30 minutes, the sample was removed, rinsed with methanol, and dried in air. Where thicker films were desired, this procedure could be repeated with fresh $Zn(NO_3)_2$ and 2-methylimidazole solutions.

Characterization and sensing experiments

The MOF/FON structures were characterized using grazing-incidence X-ray diffraction (Rigaku ATX-G) and scanning electron microscopy (Hitachi S-4800-II SEM). Plasmon resonance (UV-vis) spectra were recorded using a fiber-coupled spectrometer (SD 2000, Ocean Optics) in reflectance mode.

SERS spectra were recorded under excitation at 785 nm using a Ti:sapphire laser (Spectra Physics model 3900) coupled to a solid state pump laser (Millennia, Spectra Physics). A 785 nm band pass filter and neutral density filters were used to reject stray pump laser light and attenuate the output power at 785 nm to 1 mW (schematic in ESI†). The excitation laser was focused to a ~1 mm spot on the sample. Scattered light was collected in a 180° backscattering geometry and passed through a 785 nm notch filter before entering the spectrometer with liquid

nitrogen-cooled CCD (Princeton Instruments). Integration time for all SERS spectra was 10 s.

Vapors were introduced by either of two methods: (1) incubating the bare FONs or MOF/FONs in a sealed vial containing a liquid reservoir or (2) continuously dosing the vapor diluted in N_2 carrier gas using a Model 1010 Gas Diluter (Custom Sensor Solutions). For the continuous dosing experiments, a saturated vapor sample was prepared in N_2 in a gas sampling bag. Using the gas diluter, this saturated vapor was mixed with pure N_2 to achieve the desired vapor concentration. The diluted vapor was delivered at a constant flow rate to the sample which was housed in a stainless steel flow cell.

Results and discussion

In order to demonstrate the role of the MOF film in trapping VOCs, all SERS measurements were made in parallel on both bare Ag FON surfaces and on ZIF-8 coated FONs. SEM images of the bare Ag FON and MOF/FON are shown in Fig. 1. As shown in Fig. 1B, the ZIF-8 film forms as many small crystallites that cover the curved surfaces of the plasmonic film. This polycrystalline film morphology is very similar to the structure seen when ZIF-8 is grown on flat Si.[56] The composition of the film was confirmed to be ZIF-8 using X-ray diffraction (ESI†).

The frequency of the FON LSPR is an important factor in defining the SERS enhancement.[57] Ideally, the plasmon resonance peak should span the SERS excitation frequency and the frequency of the Raman scattered photon to achieve the highest signal for a non-resonant molecule. The plasmon resonance frequency of a FON is most easily controlled by selecting the diameter of the underlying nanospheres, with increasing sphere diameter yielding plasmon resonances at lower energy.[53] Here, both bare FON and MOF/FON substrates were optimized for SERS excitation at 785 nm. For bare FON samples, a 200 nm Ag film over 590 nm silica spheres yielded a plasmon resonance peak of 782 nm (Fig. 2). Because the deposition of the MOF film significantly shifts the plasmon resonance, the ZIF-8 was deposited on 200 nm Ag films over 390 nm silica spheres. The plasmon resonance peak of these films shifted from 580 nm (without MOF) to 762 nm with MOF growth (Fig. 2). This large shift is very reproducible and is similar to the magnitude of shift observed when placing a FON in aqueous pyridine solution (165 nm shift).[58]

Initial vapor sensing experiments showed the versatility of this sensor for detecting a range of structurally-related VOCs. Using a common method to expose the samples, bare FONs and

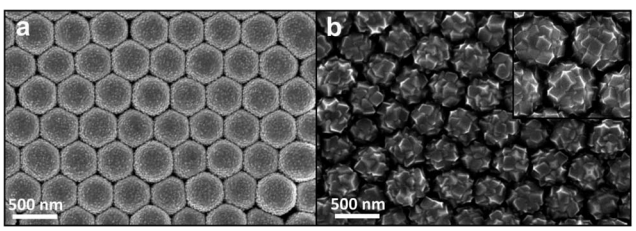

Fig. 1 SEM image of (a) AgFON and (b) ZIF-8-coated Ag FON.

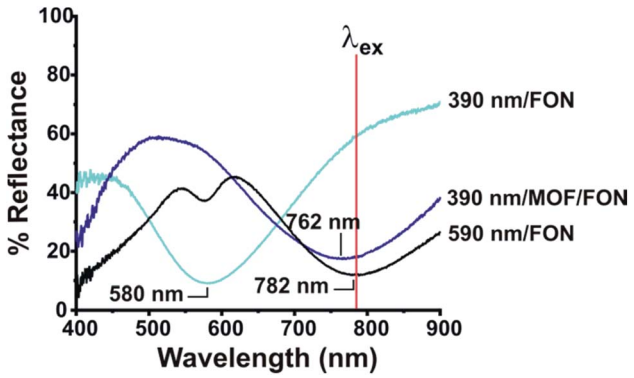

Fig. 2 UV-vis spectra recorded in reflectance geometry showing LSPR peak locations of SERS sensors: Ag FON on 590 nm diameter SiO_2 spheres (λ_{max} = 782 nm) and Ag FON on 390 nm diameter SiO_2 spheres before (λ_{max} = 580 nm) and after (λ_{max} = 762 nm) growing MOF film. Vertical line indicates excitation wavelength for SERS sensing.

MOF/FONs were incubated overnight in separate sealed vials containing a reservoir of toluene, benzene, pyridine, nitrobenzene, or 2,6-di-*tert*-butylpyridine (TBP) liquid. The FONs were mounted in the headspace above the liquid. A Raman spectrum of each sample was quickly recorded after removing it from the vapor-filled container. As shown in Fig. 3, Raman signals from each of the analytes can be detected using the MOF/FON sensors. Peak assignments for the MOF itself are provided in the "air" spectrum and correspond to vibrational modes of the organic ligand.[59] While the MOF/FON does not seem to preferentially bind or detect one of these molecules over the others, they can still be distinguished by the spectral separation of the different Raman features (relevant peaks for each species are labeled in Fig. 3). This is an obvious advantage over other sensor types that do not report on the molecular identity of adsorbates. In contrast, the bare FON samples (not shown) did not exhibit SERS spectra of any of the analytes except for pyridine using this incubation method. When the MOF film is present, it can trap the vapors at the FON surface long enough for them to be

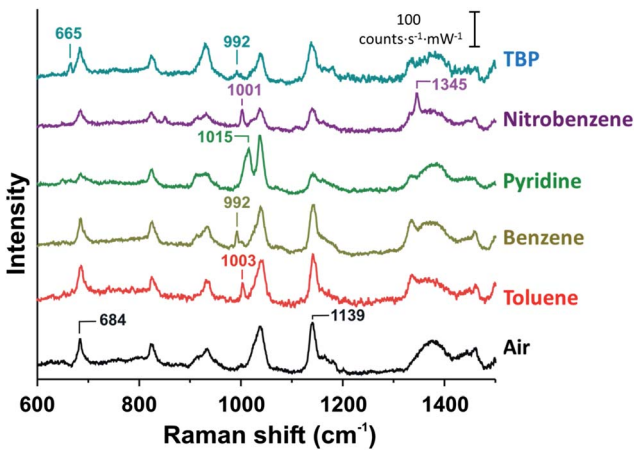

Fig. 3 SERS spectra (λ_{ex} = 785 nm) of volatile organic molecules in ZIF-8/AgFON. Characteristic peaks are labeled.

measured, but without a MOF film on top of the Ag surface, there is nothing to trap molecules in the SERS-active region. The exception to this rule is pyridine, which can chemically bind to the silver surface, and it is detected even without a MOF film. Surprisingly, nitrobenzene was not observable with the bare FON, although numerous studies of SERS detection of dinitrotoluene demonstrate that binding to Ag nanoparticles can occur through the nitro group.[60,61] In the case of Ag colloids, this binding probably stems from an interaction with the surface capping ligands, which are absent in our FON structure.

To study the response of the SERS intensity as a function of vapor concentration, separate measurements were carried out by continuously dosing the sample with increasing concentrations of the vapor in N_2 carrier gas. Fig. 4a shows the MOF/FON response to benzene with the signature ring breathing mode at 992 cm^{-1} growing in as the concentration was increased in 10% increments. In Fig. 4b the normalized intensity of this peak is plotted as a function of concentration dosed. The shape of the plot shows saturation behavior, indicating that the benzene interacts strongly with the MOF film. By comparison, Fig. 4c shows the sensor response for a bare FON. The plot is linear, demonstrating no adsorption to the surface. It is well established that benzene does not adsorb on Ag surfaces at room temperature.[29–31] We hypothesize that the SERS signal observed with the bare FON (which was *not* observed for the incubated sample) results from the formation of a layer of liquid benzene on the metal surface. The thickness of this layer (*i.e.*, number of scatterers) was calculated by comparing the benzene peak intensity with the intensity observed from a monolayer of benzenethiol adsorbed on an identical FON surface, where the surface density of the adsorbate is well known. We estimate that the signal observed with saturated benzene vapor ($p/p_0 = 1$) results from a liquid layer ~1.8 nm thick (see ESI† for details). Similar results were obtained with toluene, with saturation behavior for the MOF/FON and a linear dependence for the bare FON surface.

From the data in Fig. 4b, the limit of detection (LOD) was estimated to be 540 ppm by fitting a line to the first two data points (an underestimation based on the observed saturation behavior) and interpolating the lowest measureable value based on a signal: noise of 3 : 1. This concentration does not yet approach the exceptional LODs achieved for Ag-adsorbing analytes such as DNT or benzenethiol. These often have LODs in the low ppb range[15,61] but can be sub-ppt when drop-cast from solution.[62] Our comparatively high LOD shows that further optimization of the experimental parameters would be required for trace level detection, but we do not believe this is an inherent limitation of the MOF film as a sorbent.

Dilute concentrations of nitrobenzene and TBP could not be detected with any of the bare FON or MOF/FONs we tested under continuous dosing conditions, even at long dosing times (~1 hour). Saturated vapors of nitrobenzene and TBP could be detected, but only when the ZIF-8 film was present. The difficulty with detecting these two analytes is probably due to their low vapor pressure compared to the other molecules. The results with continuous dosing of pyridine were much more complicated, as two sets of peaks were observed: one corresponding to chemisorbed pyridine and one corresponding to liquid-like or physisorbed pyridine. The peaks showed different dependences on concentration, making the interpretation less straightforward. To summarize, all analytes could be detected using the incubation method when a MOF film was present, but only pyridine was detected if the MOF film was not present. Similarly, all analytes could be detected under continuous dosing experiments when the MOF film was present, but only toluene, benzene, and pyridine could be detected without the MOF film. These results highlight the importance of the MOF film for concentrating and trapping the vapors.

To further test our hypothesis that the ZIF-8 film traps VOCs at the FON surface, we compared the desorption kinetics in MOF/FONs with the bare FON surface. For this purpose, the decay of the benzene and toluene signals from both ZIF-8-coated and bare FONs was measured. At the start of the measurement, 80% vapor was flowing to the sample using the gas diluter, and at time = 0, the gas diluter was switched to deliver pure N_2 to purge out the vapor. A spectrum was collected every two minutes throughout the purging. Fig. 5A shows the decrease of the peak intensity at 1003 cm^{-1} as 80% toluene vapor was being purged from the sample cell containing either the bare FON or MOF/FON. Note that the peak intensity is normalized to the intensity at time = 0 min to show both on the same plot.

When the sensor was coated with a ZIF-8 film (red), the signal decayed slowly due to very slow desorption of the toluene. Typically, overnight purging was required to return to a baseline value. However, with a bare FON surface (blue), the toluene was

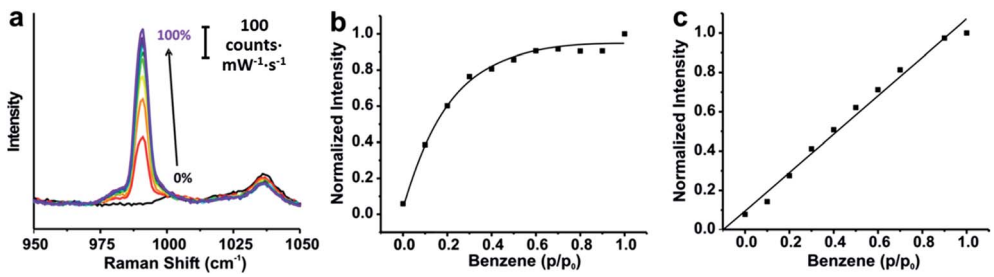

Fig. 4 (a) Series of spectra of ZIF-8/AgFON during dosing of increasing concentrations of benzene vapor showing peak appearing at 992 cm^{-1}. Normalized peak intensity at 992 cm^{-1} as a function of benzene concentration dosed on (b) ZIF-8/AgFON and (c) bare AgFON. Lines in b and c are provided as a guide to the eye.

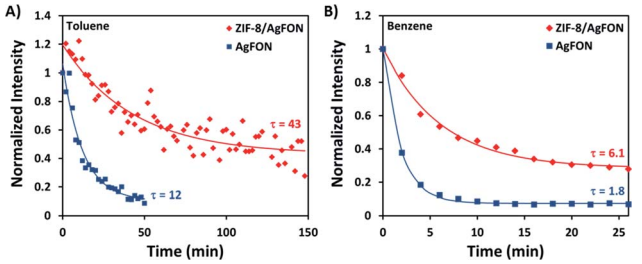

Fig. 5 (A) Desorption of toluene from ZIF-8 coated (diamonds) and bare (squares) FONs shown by the normalized peak intensity at 1003 cm^{-1}. (B) Desorption of benzene from ZIF-8 coated (diamonds) and bare (squares) FONs shown by the normalized peak intensity at 992 cm^{-1}. Each point represents one spectrum, and lines represent the fit of a first order exponential decay to the data.

removed much more rapidly. When both of these plots were fit to a first order exponential decay (eqn (1)), τ_{MOF} for the ZIF-8 coated sensor was 43 minutes, while τ_{bare} for the bare FON was only 12 minutes.

$$y = y_0 + e^{-t/\tau} \quad (1)$$

Similar results were obtained for benzene by measuring the intensity at 992 cm^{-1}, shown in Fig. 5B, where $\tau_{MOF} = 6.1$ min and $\tau_{bare} = 1.8$ min. Thus, for both vapors τ_{MOF} is ~3.5 times τ_{bare}. Although the vapors appear to condense on the bare FON surface under these conditions, they are not strongly adsorbed and diffuse away very rapidly. By contrast, the MOF film retains vapor substantially longer. It is likely that for the bare FON, the signal decay time is indicative of how long it takes to thoroughly purge the vapor diluter and sample flow cell of the test vapor. It is unclear why benzene is removed from the diluter faster than toluene (as indicated by the bare sensors); this may be due to some adsorption of toluene on the components of the diluter itself.

These results are consistent with our previous observation that the VOCs are detected in the MOF/FON but not the bare FON when incubated in pure vapor overnight. In the case of the bare FON, the vapors are not adsorbed or trapped at the metal surface, and so they quickly diffuse away when the sample is removed from the vial containing the vapor. By the time the SERS spectrum is collected (~60 s later), no vapor remains. However, the ZIF-8 film absorbs and traps the analyte molecules long enough for them to be identified.

Initially, the evidence of absorption of these vapors by the ZIF-8 film was unexpected. Typically, uptake of guests is dominated by adsorption in the MOF micropores. However, all of these molecules have larger dimensions than the ZIF-8 pore aperture (3.4 Å), so they are not expected to enter the MOF micropores.[55] In the MOF literature there has been some debate about the pore size of ZIF-8 in particular. Fairen-Jimenez *et al.* showed that dynamic simulations, which allow some movement of MOF linkers, predict a more expanded aperture than was previously assumed from crystal structure data where the framework is rigid.[63] However, even the larger pore size calculated computationally could not accommodate all of the molecules we have been able to detect in ZIF-8 films. Furthermore, Demessence *et al.* have reported that a film of ZIF-8 nanocrystals showed little uptake of toluene by ellipsometric porosimetry.[64] Yet another experimental report suggests that benzene *is* absorbed in ZIF-8 membranes.[65] While we do not claim that the vapors tested in this work are infiltrating the MOF micropores, it does seem plausible that the molecules are absorbed in larger mesopores that form at grain boundaries in our films; SEM images show that the films are highly polycrystalline.

Luebbers *et al.* reported interesting results on the adsorption of volatile organics in ZIF-8 as studied by inverse gas chromatography. Though they note that aromatic molecules, such as toluene, are not significantly retained by the bulk ZIF-8, they observe a significant tailing effect that is attributed in part to "strong interactions with the ZIF crystals' exposed surfaces."[55] If this interpretation is correct, it might explain why we observe strong interactions between aromatic molecules and ZIF-8. We speculate that the nanocrystalline ZIF-8 films probably have significant amounts of "surface" exposed at the grain boundaries, providing a greatly increased surface area available for interacting with vapors when compared to bulk materials which have a smaller fraction of external surface area. Further evidence that vapors are absorbed throughout the thickness of the MOF film (rather than on the top surface or between the MOF film and FON only) was found by measuring the uptake of pyridine in ZIF-8 films using quartz crystal microbalance gravimetry. These measurements showed that the amount of vapor absorbed scales with the thickness of the film (ESI†).

Analysis of the MOF Raman spectrum lends further evidence that this vapor sorption is reversible. We can take the case of benzene absorption as an example. Analysis of the peak at 685 cm^{-1}, which corresponds to a MOF Raman peak, shows that there is a decrease in the intensity of the MOF signal correlated with the increase of the benzene peak intensity at 992 cm^{-1}. A loss of intensity could indicate a loss of MOF material; however Park *et al.* have shown that ZIF-8 is stable even to boiling liquid benzene,[54] so this explanation seems unlikely. SEM analysis also shows that the structure is maintained after exposure to the vapor (ESI†). Furthermore, when benzene is flushed out of the flow cell, the intensity of the MOF peak concurrently recovers, although not to its initial value. The correlation between the changes in benzene and MOF signals could result from some swelling of the film which moves some of the MOF outside of the 2–3 nm SERS-active hot spots at the FON surface. Though ZIFs are generally viewed as rigid structures, the polycrystallinity of the film could potentially lead to different behavior. Absorption of benzene beneath the MOF film, between the MOF and the FON, would also be consistent with the observed fall and rise of the MOF Raman signal, as this could also increase the distance between the MOF and the FON surface. We have grown ZIF-8 films using a self-assembled monolayer (SAM) to covalently bind the ZIF-8 film to the underlying Ag surface, and benzene is still detected, although the Raman intensity is lower than without the SAM. While this cannot entirely rule out the possibility that there is some vapor trapped between the MOF and Ag FON, the SAM experiment

suggests this cannot be the only mechanism of trapping vapor. This is also supported by our quartz crystal microbalance measurements.

The above explanations for the changes in the MOF peak intensity are consistent with reversible vapor absorption, but the most likely cause is a change in the refractive index of the MOF film as vapors are absorbed and desorbed. This can shift the LSPR of the FON in and out of resonance with the Raman excitation laser and cause changes in the SERS enhancement. The reversibility of the MOF SERS intensity suggests that the change in refractive index (and hence absorption of vapor) is reversible.

One other possible explanation for the observed analyte spectra from MOF/FONs could be simple normal Raman scattering of pre-concentrated molecules in the MOF, rather than any effect of surface enhancement. To test this possibility, ZIF-8 films were grown directly on nanospheres, with no intermediate Ag layer, thus removing the possibility of surface enhancement. This as-made sample showed no Raman peaks corresponding to the ZIF-8 film (Fig. 6d). When dosed with pyridine, it likewise showed no pyridine Raman spectrum (Fig. 6c). For comparison, the spectra of the ZIF-8 film with underlying Ag film are also shown in Fig. 6.

Another way to test the contributions of normal Raman scattering *versus* SERS is to compare films of different thicknesses. To do this, the typical ZIF-8 film synthesis was performed on two FON sensors. One MOF/FON was left as made, with one "layer" of ZIF-8; on the second sample, the ZIF-8 growth was repeated four more times using new precursor solutions each time, forming a film that was five times as thick as the single layer film. If normal Raman scattering is the primary mechanism of these sensors, then the thicker film should absorb five times as much analyte and therefore have a five times stronger Raman signal than the thinner film. If SERS is primarily responsible, as we hypothesized, then the majority of the signal originates from analytes within a few nanometers of the metal surface (much closer than the thickness of either one- or five-layer films), so the two films should produce nominally the same adsorbate Raman signal. We found that, for a benzene sensing experiment, the thicker film actually produced a $\sim 2\times$ weaker benzene Raman signal than the thinner film. This implies that normal Raman scattering of benzene absorbed in the bulk of the film is not a major contributor to the observed signal. The weaker signal could indicate that it is more difficult for vapors to penetrate through the thicker film to the FON surface. Combined with the previous experiment showing no signal in the absence of a plasmonic film, this result confirms that the observation of analyte spectra from the MOF/FON sensor must require surface enhancement.

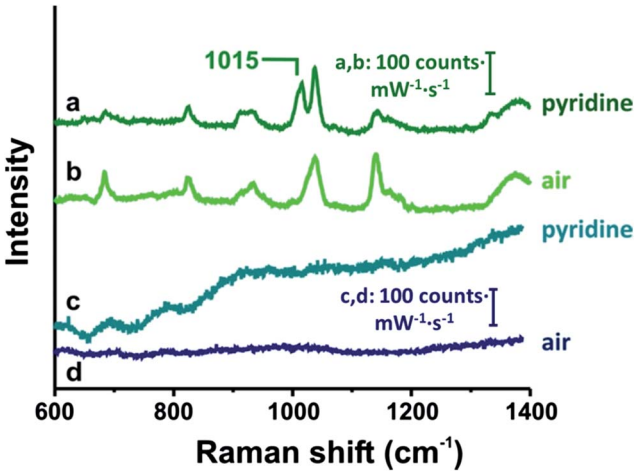

Fig. 6 SERS spectra of ZIF-8/AgFON after (a) and before (b) incubating in pyridine, showing a peak centered at 1015 cm^{-1} due to pyridine in the incubated sample (a). Spectra of ZIF-8 film only, without Ag film after (c) and before (d) incubating in pyridine.

Conclusion

We have demonstrated an entirely new approach to functionalizing Ag FONs with MOF films to reversibly bind organic molecules within the sensing volume of SERS using polarizability interactions. This concept builds off of our previous work coupling MOFs with plasmonic nanoparticles to make refractive index-based sensors. Here, we were able to not only detect the presence of small aromatic molecules from the vapor phase but also identify the analyte spectral information unique to each molecule. The LOD for benzene, the most rigorously studied analyte, was calculated to be 540 ppm. By contrast, conventional non-functionalized SERS substrates were unable to detect most of these analytes by incubation in the vapors. The advantage of the MOF functionalization approach lies in being able to exploit of the relatively non-specific interactions between the MOF surface and a range of VOCs to retain these molecules in close proximity to metal nanostructures.

Moreover, a compelling approach for developing future MOF sensors will be to employ MOFs with larger apertures such that the analyte can access the entire micropore volume, resulting in an even higher pre-concentration effect. Though vibrational spectroscopy obviates the need for extremely selective sorption by the MOF, future design of MOF films with high selectivity will also be an important goal for advancing MOFs as sensors. Given the tunable sorption properties that have been demonstrated using MOFs for gas separations, the potential for molecular recognition by MOFs in principle gives them an obvious advantage over other sensor materials, but this has yet to be exploited.

Through the surprising observation that ZIF-8 thin films were able to adsorb molecules much larger than the 3.4 Å apertures, we have also highlighted an unintentional consequence of the increased external surface area present in MOF films relative to bulk materials. Our data is consistent with the hypothesis that significant adsorption is occurring on the "surface" of the MOF nanocrystallites exposed at grain boundaries in the film. Other groups have made significant efforts at making pinhole-free MOF membranes for gas separations which would block the behavior we observe. However, as film dimensions become smaller for integrating MOFs into sensors and other devices, polycrystalline structures dominate and growing pinhole-free films is a challenge. As our experiments

suggest, the prevalence of inter-particle spaces may translate to sorption properties that are dominated by interparticle mesopores rather than the targeted MOF micropores. This unexpected result has important implications for the use of MOF films for selective sensing and other device applications.

Acknowledgements

This work was supported by the Defense Threat Reduction Agency (HDTRA 1-09-1-0007), the National Science Foundation (CMI CHE-1152547), and the Department of Defense (NDSEG) and National Science Foundation (GRFP) student fellowships (LEK).

References

1 F. Yan and T. Vo-Dinh, *Sens. Actuators, B*, 2007, **121**, 61–66.
2 M. A. Young, D. A. Stuart, O. Lyandres, M. R. Glucksberg and R. P. Van Duyne, *Can. J. Chem.*, 2004, **82**, 1435–1441.
3 K. Kneipp, Y. Wang, H. Kneipp, L. T. Perelman, I. Itzkan, R. R. Dasari and M. S. Feld, *Phys. Rev. Lett.*, 1997, **78**, 1667–1670.
4 S. M. Nie and S. R. Emery, *Science*, 1997, **275**, 1102–1106.
5 J. A. Dieringer, R. B. Lettan, K. A. Scheidt and R. P. Van Duyne, *J. Am. Chem. Soc.*, 2007, **129**, 16249–16256.
6 E. J. Blackie, E. C. Le Ru and P. G. Etchegoin, *J. Am. Chem. Soc.*, 2009, **131**, 14466–14472.
7 B. Sharma, R. R. Frontiera, A.-I. Henry, E. Ringe and R. P. Van Duyne, *Mater. Today*, 2012, **15**, 16–25.
8 S. L. Kleinman, B. Sharma, M. G. Blaber, A.-I. Henry, N. Valley, R. G. Freeman, M. J. Natan, G. C. Schatz and R. P. Van Duyne, *J. Am. Chem. Soc.*, 2012, **135**, 301–308.
9 M. Rycenga, X. H. Xia, C. H. Moran, F. Zhou, D. Qin, Z. Y. Li and Y. A. Xia, *Angew. Chem., Int. Ed.*, 2011, **50**, 5473–5477.
10 A. Campion and P. Kambhampati, *Chem. Soc. Rev.*, 1998, **27**, 241–250.
11 D. L. Jeanmaire and R. P. V. Duyne, *J. Electroanal. Chem.*, 1977, **84**, 1–20.
12 S. L. Kleinman, E. Ringe, N. Valley, K. L. Wustholz, E. Phillips, K. A. Scheidt, G. C. Schatz and R. P. Van Duyne, *J. Am. Chem. Soc.*, 2011, **133**, 4115–4122.
13 W. W. Yu and I. M. White, *Analyst*, 2013, **138**, 1020–1025.
14 K. B. Biggs, J. P. Camden, J. N. Anker and R. P. Van Duyne, *J. Phys. Chem. A*, 2009, **113**, 4581–4586.
15 R. Kodiyath, S. T. Malak, Z. A. Combs, T. Koenig, M. A. Mahmoud, M. A. El-Sayed and V. V. Tsukruk, *J. Mater. Chem. A*, 2013, **1**, 2777–2788.
16 S. S. R. Dasary, A. K. Singh, D. Senapati, H. Yu and P. C. Ray, *J. Am. Chem. Soc.*, 2009, **131**, 13806–13812.
17 X. Fang and S. R. Ahmad, *Appl. Phys. B: Lasers Opt.*, 2009, **97**, 723–726.
18 J. C. Santos Costa, R. A. Ando, A. C. Sant'Ana, L. M. Rossi, P. S. Santos, M. L. A. Temperini and P. Corio, *Phys. Chem. Chem. Phys.*, 2009, **11**, 7491–7498.
19 J. M. Yu and P. B. Balbuena, *J. Phys. Chem. C*, 2013, **117**, 3383–3388.
20 N. Taranenko, J.-P. Alarie, D. L. Stokes and T. Vo-Dinh, *J. Raman Spectrosc.*, 1996, **27**, 379–384.
21 T. Vo-Dinh and D. L. Stokes, *Field Anal. Chem. Technol.*, 1999, **3**, 346–356.
22 J. Du and C. Jing, *J. Phys. Chem. C*, 2011, **115**, 17829–17835.
23 M. Litorja, C. L. Haynes, A. J. Haes, T. R. Jensen and R. P. Van Duyne, *J. Phys. Chem. B*, 2001, **105**, 6907–6915.
24 R. A. Wolkow and M. Moskovits, *J. Chem. Phys.*, 1992, **96**, 3966–3980.
25 M. Moskovits and D. P. Dilella, *J. Chem. Phys.*, 1980, **73**, 6068–6075.
26 O. Lyandres, N. C. Shah, C. R. Yonzon, J. T. Walsh, M. R. Glucksberg and R. P. Van Duyne, *Anal. Chem.*, 2005, **77**, 6134–6139.
27 L. A. Dick, A. J. Haes and R. P. Van Duyne, *J. Phys. Chem. B*, 2000, **104**, 11752–11762.
28 H. Ko and V. V. Tsukruk, *Small*, 2008, **4**, 1980–1984.
29 F. P. Netzer, *Langmuir*, 1991, **7**, 2544–2547.
30 P. Avouris and J. E. Demuth, *J. Chem. Phys.*, 1981, **75**, 4783–4794.
31 T. J. Rockey, M. Yang and H.-L. Dai, *J. Phys. Chem. B*, 2006, **110**, 19973–19978.
32 K. T. Carron and B. J. Kennedy, *Anal. Chem.*, 1995, **67**, 3353–3356.
33 P. A. Mosier-Boss and S. H. Lieberman, *Anal. Chim. Acta*, 2003, **488**, 15–23.
34 D. L. Stokes, A. Pal, V. Anantha Narayanan and T. Vo-Dinh, *Anal. Chim. Acta*, 1999, **399**, 265–274.
35 S. Chang, H. Ko, S. Singamaneni, R. Gunawidjaja and V. V. Tsukruk, *Anal. Chem.*, 2009, **81**, 5740–5748.
36 S. Kitagawa, R. Kitaura and S. Noro, *Angew. Chem., Int. Ed.*, 2004, **43**, 2334–2375.
37 G. Férey, *Chem. Soc. Rev.*, 2008, **37**, 191–214.
38 D. J. Tranchemontagne, J. L. Mendoza-Cortes, M. O'Keeffe and O. M. Yaghi, *Chem. Soc. Rev.*, 2009, **38**, 1257–1283.
39 O. K. Farha, I. Eryazici, N. C. Jeong, B. G. Hauser, C. E. Wilmer, A. A. Sarjeant, R. Q. Snurr, S. T. Nguyen, A. Ö. Yazaydın and J. T. Hupp, *J. Am. Chem. Soc.*, 2012, **134**, 15016–15021.
40 R. B. Getman, Y.-S. Bae, C. E. Wilmer and R. Q. Snurr, *Chem. Rev.*, 2012, **112**, 703–723.
41 M. P. Suh, H. J. Park, T. K. Prasad and D.-W. Lim, *Chem. Rev.*, 2012, **112**, 782–835.
42 K. Sumida, D. L. Rogow, J. A. Mason, T. M. McDonald, E. D. Bloch, Z. R. Herm, T.-H. Bae and J. R. Long, *Chem. Rev.*, 2012, **112**, 724–781.
43 J.-R. Li, J. Sculley and H.-C. Zhou, *Chem. Rev.*, 2012, **112**, 869–932.
44 M. Ranocchiari and J. A. van Bokhoven, *Phys. Chem. Chem. Phys.*, 2011, **13**, 6388–6396.
45 M. Yoon, R. Srirambalaji and K. Kim, *Chem. Rev.*, 2012, **112**, 1196–1231.
46 B. L. Chen, S. C. Xiang and G. D. Qian, *Acc. Chem. Res.*, 2010, **43**, 1115–1124.
47 L. E. Kreno, K. Leong, O. K. Farha, M. Allendorf, R. P. Van Duyne and J. T. Hupp, *Chem. Rev.*, 2011, **112**, 1105–1125.

48 L. E. Kreno, J. T. Hupp and R. P. Van Duyne, *Anal. Chem.*, 2010, **82**, 8042–8046.
49 K. Sugikawa, Y. Furukawa and K. Sada, *Chem. Mater.*, 2011, **23**, 3132–3134.
50 R. P. Vanduyne, J. C. Hulteen and D. A. Treichel, *J. Chem. Phys.*, 1993, **99**, 2101–2115.
51 W.-C. Lin, L.-S. Liao, Y.-H. Chen, H.-C. Chang, D. P. Tsai and H.-P. Chiang, *Plasmonics*, 2011, **6**, 201–206.
52 C. Farcau and S. Astilean, *J. Phys. Chem. C*, 2010, **114**, 11717–11722.
53 N. G. Greeneltch, M. G. Blaber, A.-I. Henry, G. C. Schatz and R. P. Van Duyne, *Anal. Chem.*, 2013, **85**, 2297–2303.
54 K. S. Park, Z. Ni, A. P. Cote, J. Y. Choi, R. Huang, F. J. Uribe-Romo, H. K. Chae, M. O'Keeffe and O. M. Yaghi, *Proc. Natl. Acad. Sci. U. S. A.*, 2006, **103**, 10186–10191.
55 M. T. Luebbers, T. J. Wu, L. J. Shen and R. I. Masel, *Langmuir*, 2010, **26**, 15625–15633.
56 G. Lu and J. T. Hupp, *J. Am. Chem. Soc.*, 2010, **132**, 7832–7833.
57 A. D. McFarland, M. A. Young, J. A. Dieringer and R. P. Van Duyne, *J. Phys. Chem. B*, 2005, **109**, 11279–11285.
58 K. Kosuda, *Ph.D. Thesis*, Northwestern University, 2010.
59 D. A. Carter and J. E. Pemberton, *J. Raman Spectrosc.*, 1997, **28**, 939–946.
60 B. D. Piorek, S. J. Lee, M. Moskovits and C. D. Meinhart, *Anal. Chem.*, 2012, **84**, 9700–9705.
61 M. K. K. Oo, C. F. Chang, Y. Z. Sun and X. D. Fan, *Analyst*, 2011, **136**, 2811–2817.
62 H. Ko, S. Chang and V. V. Tsukruk, *ACS Nano*, 2009, **3**, 181–188.
63 D. Fairen-Jimenez, S. A. Moggach, M. T. Wharmby, P. A. Wright, S. Parsons and T. Düren, *J. Am. Chem. Soc.*, 2011, **133**, 8900–8902.
64 A. Demessence, C. Boissiere, D. Grosso, P. Horcajada, C. Serre, G. Ferey, G. J. A. A. Soler-Illia and C. Sanchez, *J. Mater. Chem.*, 2010, **20**, 7676–7681.
65 L. Diestel, H. Bux, D. Wachsmuth and J. Caro, *Microporous Mesoporous Mater.*, 2012, **164**, 288–293.